Determination of the AISI 1045 steel ablation threshold dependence on the pulse superposition using the Diagonal Scan (D-Scan) technique

Ricardo E. Samad*, Denilson C. Mirim, Wagner de Rossi, Nilson D. Vieira Jr.
IPEN-CNEN/SP – Av. Prof. Lineu Prestes 2242, São Paulo, SP, Brazil, 05508-000

ABSTRACT

We report the use of the Diagonal Scan (D-Scan) technique to determine the ablation threshold of the AISI 1045 steel, a common engineering material that can be used as a probe for thermal effects, for superpositions ranging from single shot up to more than 10,000 pulses, for three pulses durations (25, 87 and 124 fs). It only took two hours of laboratory time to determine more than 20 ablation thresholds per pulse duration spanning 4 orders of magnitude of superpositions. The large amount of data generated shows a small deviation of the ablation threshold from the expected behavior, which can lead to the use of a model that better describes the dynamics of the ultrashort pulses ablation mechanism in metals.

Keywords: Femtosecond Ablation, Diagonal Scan, Ablation Threshold, AISI 1045 Steel, Incubation Effects.

1. INTRODUCTION

Over the last years, the need for micromachining technologies boosted the growth of scientific research directed to the manufacturing sector. Segments of the medical, microelectronic and automotive world provided a wide variety of applications for this technology, such as the production of micromotors, microfluidic circuits, MEMS (Micro Electrical Mechanical System), medical devices, electronic tools, particle filters, micromolds and microvalves, among others[1]. This huge growth in this segment requires a variety of new micromachining methods.

Techniques for machining the surface of materials are being continuously improved and among them, laser etching is a widely used method. The dimensions of the structures that can be machined with the laser depend, in the first approximation, on the focused beam diameter but the final processed area depends on the heat diffusion volume guided by the process dynamics. When a laser pulse is absorbed, the material is heated and thermodynamic processes regulate the thermal diffusion and phase transformations that culminate into material ejection. The excess heat not directly used in the ablation neither carried by the ejected material flows into the surroundings increasing its temperature, and eventually creating a Heat Affected Zone (HAZ), in which phase transitions modify the material properties, usually in an uncontrolled and, therefore, detrimental way. As the laser pulse shortens higher intensities are reached faster, the spatial heat propagation is decreased, phase transformations that result in ablation occur more efficiently[2], and the HAZ is decreased. Besides decreasing the heat propagation and minimizing the HAZ, ultrashort pulses present unique advantageous characteristics to etch different materials[3].

The ablation by ultrashort pulses is due to a Coulomb explosion[4, 5] following the ejection of surface electrons accelerated by the laser electric field, or by a phase explosion[6-8] resulting from in a high density of free electrons[9, 10] generated by avalanche ionization[11]. The pulses very brief duration, shorter than the typical phonon period, mainly heats the electrons[12, 13], and the explosions that remove material occur after the pulse has finished, with minimal material heating. The avalanche occurs when seed electrons, either already present in metals or created by tunneling[14] or multiphoton ionization[2, 15] in other materials, are accelerated by the ultrashort pulse electric field into a quivering motion and generate more free electrons by impact ionization[11] in an exponential growth process that is almost independent of the material being irradiated. The high intensities reached by ultrashort pulses easily induce the nonlinear phenomena that create the initial free electrons, making these pulses efficient tools to etch any kind of material[3]. Due to this nonselective mechanism, the only parameter that has to be known to etch a material with ultrashort pulses is its ablation threshold fluence, F_{th}.

The ultrashort pulses ablation threshold derives from the material atoms bonding energies, electronic density and its ionizing energies, which depend on the presence of dopants, impurities or other defects[16, 17]. As a consequence of the defects presence, the seed electrons are created more easily and the avalanche ones are freed at lower impact energies,

* resamad@gmail.com; phone: +55-11-3133-9387; fax: +55-11-3133-9372

Frontiers in Ultrafast Optics: Biomedical, Scientific, and Industrial Applications XIV, edited by Alexander Heisterkamp, Peter R. Herman, Michel Meunier, Stefan Nolte, Proc. of SPIE Vol. 8972, 89721G
 · doi: 10.1117/12.2039440

decreasing the F_{th} value. The defects can be intrinsic to the material, or externally generated such as color centers created by ultrashort laser pulses[18], and in this case the modifications induced by a pulse modify the F_{th} value for the following pulses, until the defects density reaches saturation and F_{th} stabilizes at a constant value. These cumulative phenomena are known as incubation effects[19-21], and the ablation threshold fluence modifications caused by them must be taken into account when machining a material.

A few years ago we introduced a simple experimental technique, which we denominated D-Scan (Diagonal Scan), to quickly measure the ultrashort pulses ablation threshold of a solid sample[22, 23]. The method uses a focused TEM_{00} Gaussian beam and the sample, with its face aligned normally to the laser beam, is moved diagonally across the beamwaist, as schematically shown in Figure 1. The sample movement should start away from the beamwaist, at a position where the beam intensity does not ablate the sample, go through the beamwaist position, and stop after the ablation has ceased. If the pulses intensity is sufficiently high[22], the profile shown in Figure 2, with two symmetrical lobes, is etched in the sample surface. If the etched profile does not exhibit the lobes, the scan has to be performed with more energetic pulses or with a tighter focusing lens[22].

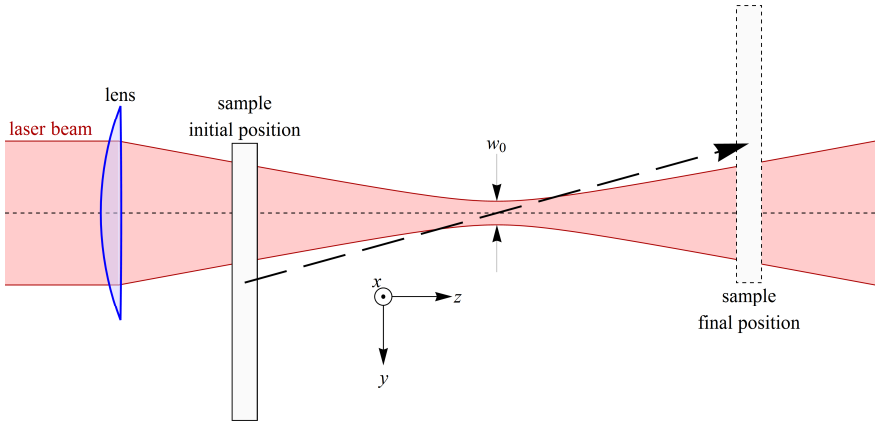

Figure 1. Scheme of the D-Scan experimental setup, top view. The dashed arrow indicates the sample diagonal movement through the beamwaist (w_0) of a focused Gaussian beam.

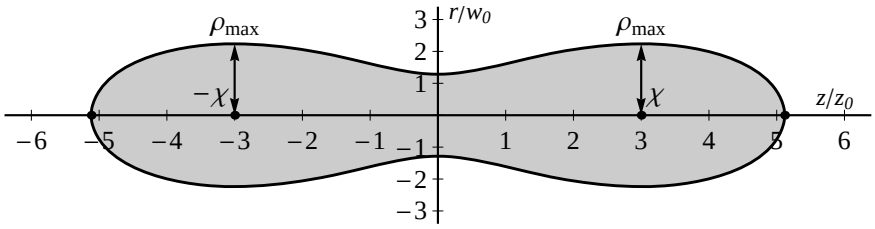

Figure 2. Scheme of the Profile ablated on the sample surface by the D-Scan technique, with maximum transversal size $2\rho_{max}$. The axes are normalized by the beamwaist (w_0) and the beam confocal parameter (z_0).

It can be shown that the ablation threshold fluence of the sample is related to the profile maximum transversal size, $2\rho_{max}$, by[22]:

$$F_{th} = \frac{1}{e\pi}\frac{E_0}{\rho_{max}^2}, \qquad (1)$$

where E_0 is the pulse energy. No parameter of the laser beam geometry has to be known, no precise sample positioning is needed, and the measurement can be quickly done. To determine the pulses superposition N that etches the profile at the ρ_{max} position, we hypothesized that it is the sum, at this position, of the intensity of all the pulses that hit the sample during the D-Scan, normalized by the intensity of the pulse centered at χ. Under this assumption, we showed that N is given by[24]:

$$N = \vartheta_3(0, e^{-\left(\frac{v_y}{f\rho_{max}}\right)^2}), \quad (2)$$

where ϑ_3 is the Jacobi theta function of the third kind[25], f is the laser repetition rate and v_y is the sample translation speed transversely to the beam (y direction in Figure 1). For high repletion rates or small displacement speeds expression (2) can be simplified to:

$$N = \sqrt{\pi}\frac{f\rho_{max}}{v_y} \approx 1.8\frac{f\rho_{max}}{v_y}. \quad (3)$$

In practical terms, equation (3) can be used at all times, but if it results in $N<2$ the superposition must be recalculated using equation (2).

Within this framework, determining the ablation threshold, F_{th}, for a sample using the D-Scan technique consists in moving the sample across the beamwaist of a focused Gaussian beam with a constant speed, then measure the ρ_{max} value under a microscope and finally use expression (1). The application of expression (3) (or expression (2)) determines the superposition for this F_{th}. The only two experimental conditions that should be met are the presence of two lobes in the profile[22] and the longitudinal and transversal displacement speeds must be such as to etch an elongated profile[24] in which the D-Scan trace width does not vary abruptly around the ρ_{max} position. To determine the F_{th} dependence on the pulses superposition, many scans have to be done with different laser repetition rates and displacement speeds.

In this work we used the D-Scan to determine the AISI 1045 steel ultrashort pulses ablation threshold dependence on the pulses superposition for three pulses duration. This steel is a widely used engineering material and can be used as a probe for thermal effects.

2. EXPERIMENTAL SETUP

The ablation threshold measurements were made on AISI 1045 medium-carbon steel[26] samples with the following composition in weight %: C (0.43-0.50), Mn (0.6-0.9), S (0.05), P (<0.045) and Fe (balance). This material is very susceptible to thermally induced phase transitions, changing from a ferrite (BCC structure) to an austenite (FCC) phase at 704 °C[26], and also presenting a melting point close to 1410 °C. The steel samples were flush mounted in Bakelite, ground and polished with 1 μm diamond paste, resulting in exposed faces measuring approximately 15×20 mm^2 (Figure 3). The ultrashort laser pulses were generated by an amplified Ti:Sapphire laser system (Femtopower Compact Pro CE-Phase HP/HR seeded by a Rainbow oscillator, both from Femtolasers), centered at 785 nm, with 37 nm of bandwidth, at 4 kHz maximum repetition rate controlled by a Pockels cell, and 800 μJ maximum pulse energy, linearly polarized in the horizontal direction. The pulses duration was altered changing the distance between the compressor prisms, and determined to be 25, 87 and 124 fs by a FROG (Swamp Optics Grenouille 8-20-USB). For the irradiations, the pulses were attenuated to 70 μJ, the beam was focused by a 75 mm focal length achromatic doublet (Thorlabs AC254-075-B), and the sample was moved by a 3-axes computer controlled translation stage (three Newport UTS100CC stages). During the scans the sample was always moved from before to after the beamwaist (away from the focusing doublet), from right to left, as indicated in Figure 1. Various combinations of repetition rates, f, and sample transversal displacement speeds, v_y (in the horizontal plane), were used to cover superpositions from single shot to more than 10^4 pulses (100, 500 and 4000 Hz and 0.05, 0.1, 0.2, 0.3, 0.4, 0.5, 1, 2, 2.5, 3, 5, 10, 20, 30 mm/s); the longitudinal sample displacement speed, v_z (in the horizontal plane), was always equal to v_y to etch elongated profiles[24]; after each D-Scan trace was etched, the sample was displaced vertically (x direction) by 400 μm, and this separation was used as a scale to measure ρ_{max} in micrographs. The samples surfaces were shrouded by a 10 l/min flux of argon during the D-Scans.

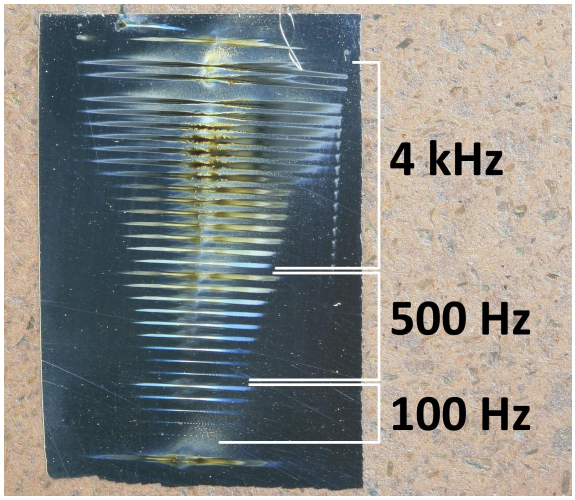

Figure 3. AISI 1045 sample flush mounted in Bakelite, exhibiting D-Scan traces etched by 25 fs pulses at different laser repetition rates and sample displacement speeds.

The photograph in Figure 3 shows more than 30 D-Scan traces engraved in a sample by 25 fs pulses. All these traces were etched in approximately 40 minutes. The two lobes, although asymmetric, can be seen in all traces. The asymmetries result from the fact that the right portion of each trace is etched when the sample is placed after the beamwaist, where the pulses generate a plasma in the air, at the beamwaist position, that distorts the beam. From top to bottom, there are two test traces, 16 traces etched at 4 kHz, 9 traces etched at 500 Hz, 5 traces at 100 Hz and a final one at 4 kHz. In the last 2 traces done at 100 Hz and high transversal displacement speeds (10 and 20 mm/s) the superposition obtained was close to 1, and individual craters can be seen.

3. RESULTS AND DISCUSSION

Figure 4 shows an optical micrograph of D-Scan traces etched by the 25 fs pulses on an AISI 1045 carbon steel sample, along with the $2\rho_{max}$ measured values. To measure these values, the 400 µm separation between traces was used as a scale for the micrograph. From these values, the ablation thresholds and pulses superpositions were calculated using eq. (1) and eq. (2), respectively, and the results for this sample are shown in the lower graph in Figure 5. The results obtained for the other temporal durations (87 fs and 124 fs) are also shown in the upper graphics on the same figure.

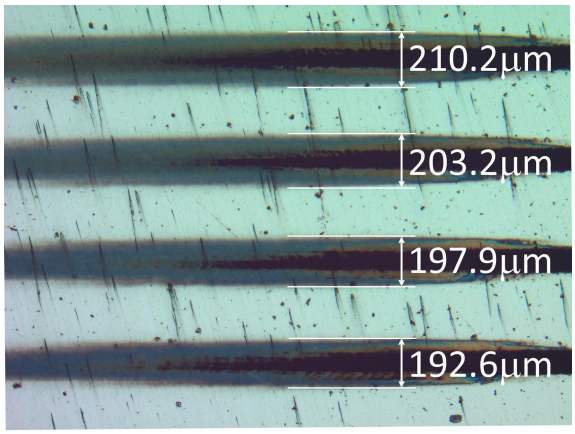

Figure 4. D-Scan traces etched on the surface of an AISI 1045 steel sample by 25 fs pulses. The 400 µm separation between the traces is used as a scale to measure $2\rho_{max}$ for each trace.

The model commonly[19, 27-29] used to account for the incubation effects in metals considers that laser pulses create defects similar to the ones originated by mechanical fatigue damage[19], resulting in an cumulative behavior described by:

$$F_{th,N} = F_{th,1} N^{S-1}, \quad (4)$$

where $F_{th,N}$ is the ablation threshold for N pulses, $F_{th,1}$ is the single shot ablation threshold and S is the sample incubation parameter. The graphs in Figure 5 also exhibit the fittings of eq. (4) to the experimental data, and the obtained values are shown in Table 1, where a slight growth of the ablation parameters ($F_{th,1}$ and S) can be observed as the pulses duration increase. This growth in both parameters is expected because as the pulses get longer their intensities decrease, requiring more energy (and fluence) to generate the nonlinear effects that result in the ablation.

Inspecting the Figure 5 graphs more closely it is possible to observe that, although the fit to the experimental points is good, some deviations from the behavior described by eq. (4) can be observed: for low (N<10) and high (N>500) superpositions, the experimental points are placed above the fitted function, and below it for intermediate values. These results indicate that eq. (4) can be considered a good approximation to describe the F_{th} dependence on N, but the model has to be improved, which is outside the scope of the present work, to correctly describe these second order deviations. Although some authors observed these deviations[28] mainly for great superpositions, they are not so noticeable on previous works[19, 27, 30, 31] that present few data points (F_{th} values), usually less than 10. This sparsity of experimental values results from the "Zero Damage" traditional method[32] used to determine F_{th}, which requires a detailed knowledge of the laser beam geometry, precise positioning of the sample and a series of measurements that can take a long experimental time, limiting the F_{th} measurements for different pulses superpositions. Using the D-Scan, many F_{th} measurements for varying N can be quickly done: all the scans (more than 80) needed to obtain the experimental data presented in Figure 5 were done in less than 2 hours of laboratory time. This is a clear advantage of the D-Scan over the traditional method.

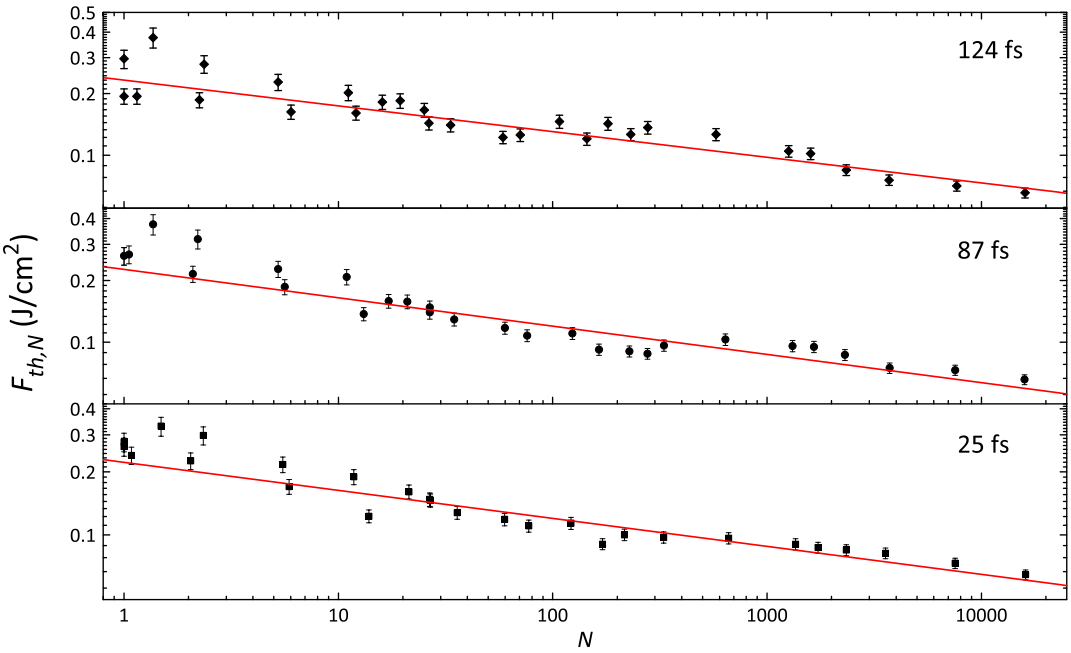

Figure 5. Log-log graphs of AISI 1045 carbon steel ablation threshold dependence on the pulses superposition, for 25, 87 and 124 fs pulses, along with fits by equation (4).

Table 1. AISI 1045 ablation parameters for three pulse durations obtained from the fits to the experimental data shown in Figure 5.

Parameter	25 fs	87 fs	124 fs
$F_{th,1}$ (J/cm^2)	0.222±0.013	0.226±0.014	0.233±0.011
S	0.866±0.010	0.862±0.011	0.874±0.008

Another advantage of the D-Scan over the traditional method relates to the machining: since the D-Scan is done in a moving sample, as in machining, its trace reproduces more closely the machining morphology for a certain superposition when compared with the traditional method, which ablates only a single spot. Under these considerations, one can determine the F_{th} for a certain superposition N and then calculate the machining parameters (beam spot-size, sample displacement speed and laser repetition rate) to process a sample with a superposition of N pulses.

To determine the superposition obtained for a sample moving in a straight line with speed v, being irradiated by a beam with spot-size w and repetition rate f, we apply our previous formalism[24] that considers that the superposition N at a specific position is the normalized intensity of the sum, at this position, of the intensity of all pulses that hit the sample. In this calculation, the beam spot-size is now constant, simplifying eq. (8) of our previous work[24], yielding that the superposition is:

$$N = \vartheta_3\left(0, e^{-2\left(\frac{v}{fw}\right)^2}\right), \tag{5}$$

that can be simplified[24], for usual machining conditions (superposition of many pulses), to:

$$N = \sqrt{\frac{\pi}{2}}\frac{fw}{v} \approx 1.25\frac{fw}{v}. \tag{6}$$

In practice, after determining the sample F_{th} for a specific superposition N, to machine the sample with this superposition using a beam with spot-size w at the sample surface, one only needs to choose the laser repetition rate f and sample displacement speed v from eq. (6).

The D-Scan provides a tool to quickly reproduce many etching conditions with varying ablation morphologies. Looking at the D-Scan traces under a SEM (Scanning Electron Microscope) many ablation regimes could be observed in our samples. Figure 6a presents a micrograph of the N=23.0 trace, taken around the χ position (Figure 2). This micrograph is representative of the traces etched from single shot up to N≈100, in which ripples oriented at 90° to the beam polarization are observed, evidencing surface modifications. These ripples, which have a 625 nm period that does not depend on the pulses superposition, modify the material reflectivity, resulting in a darkening of the steel surface that can be used for marking since at these superpositions there is almost no material removal neither severe metallurgical modifications. As the pulses superposition increase over ~100 up to ~600, the ripples break apart into a grainy structure, shown in Figure 6b, and still there is almost no material removal.

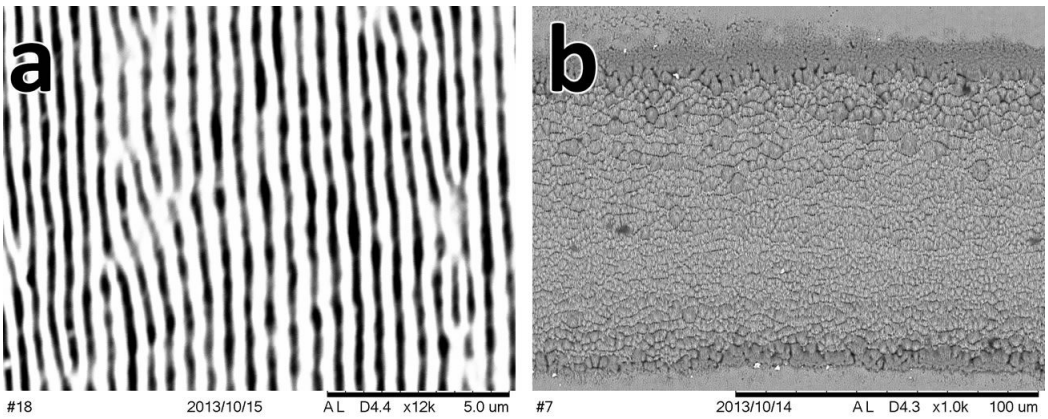

Figure 6. D-Scan traces SEM micrographs at the χ position for: a) N=23.0; b) N=577.

As the superposition increases over 1,000 there is a significant material removal and the traces exhibit a central "V" profile, as shown in Figure 7a, with an irregular bottom, without evidence of melting and material ressolidification. For N>10,000, as shown in Figure 7b, the material removal and the trace depth increase, remaining without evidence of molten material.

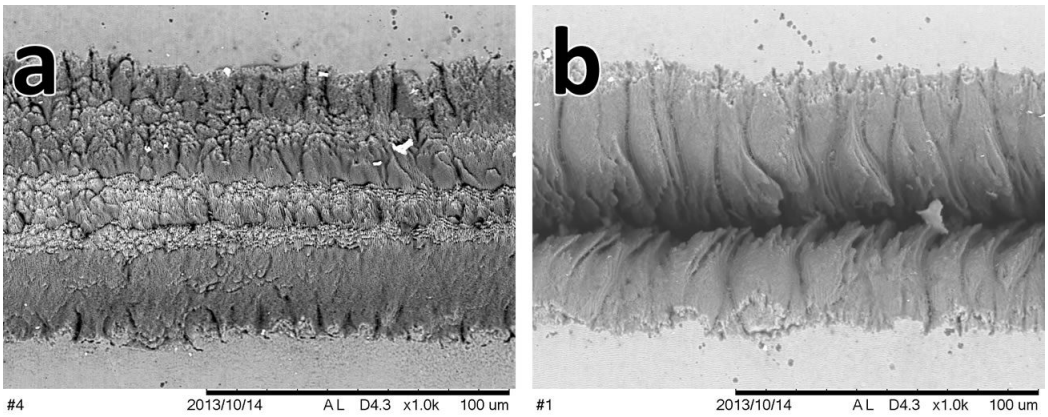

Figure 7. D-Scan traces SEM micrographs at the χ position for: a) *N*=2,059; b) *N*=14,776.

Examining the D-Scan traces at the focus position, evidence of melting and material ressolidification can be observed, even for small superpositions. Figure 8 exhibits the region around the beamwaist position (origin in Figure 2) of the *N*=9.5 trace, where ressolidifed material can be seen, evidencing that at this position the material temperature went above 1,410 °C. According to eq. (6), the superposition at the focus is smaller than the one calculated for the trace, nevertheless the melting occurs because the pulse fluence gradient is much larger at the focus than at χ[33], and the excess energy deposited by the pulse heats the material until melting occurs. This result indicates that machining a sample with fluences well above the threshold will results in a variety of morphologies in the ablated region and eventual melting that can change the material properties.

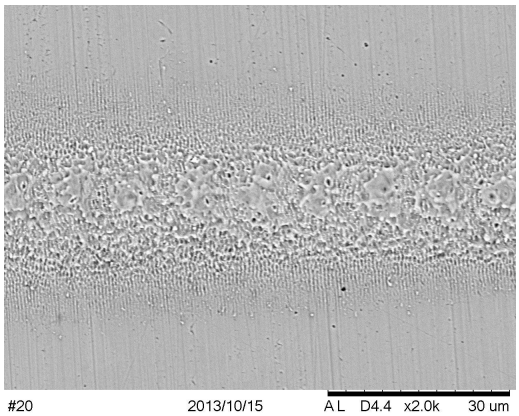

Figure 8. Melting and ressolidification observed around the focal position for the *N*=9.5 trace.

The AISI 1045 steel was chosen for this work as a probe to thermal effects during ablation by ultrashort pulses due to its sensitivity to temperature, making it a good material to investigate the extension of the HAZ. In order to do this, the traces etched by 25 fs pulses at high superpositions went under a chemical attack with Nital 3% (3% nitric acid solution in alcohol[34]) to reveal the material crystalline structure. Figure 9 shows the results near the focus position, where large amounts of material are removed, for the traces etched by 1,521 and 14,776 pulses. In these two micrographies is possible to observe the material grains, which maintain their morphology near the edge of the etching, evidencing that, if there is a HAZ, it is smaller than a few micrometers. Melting occurred, but the thermal effect did not propagate to the surrounding region. Moreover, the fact that the grains morphology remains unaltered means that no phase transition (from ferrite to austenite) occurred, meaning that the local temperature did not go over 704 °C, preserving the material properties.

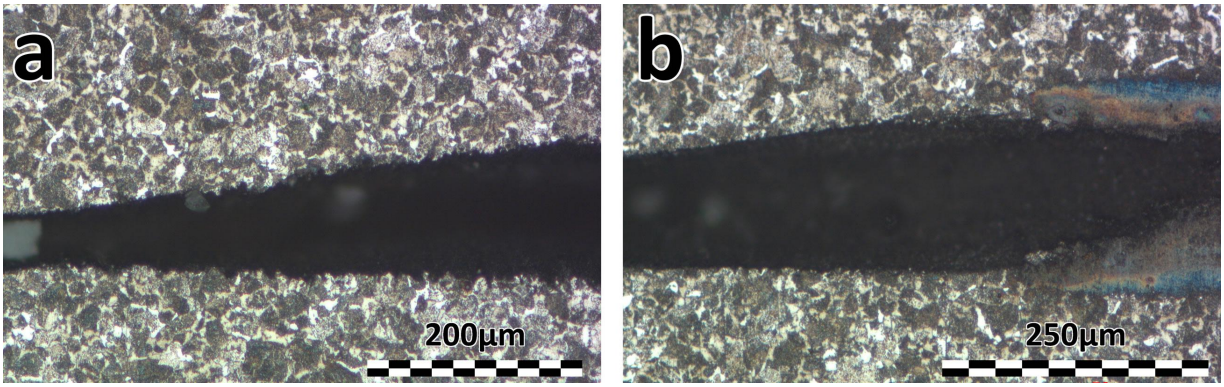

Figure 9. Optical micrographs of AISI 1050 surfaces chemically etched by Nital 3% evidencing the material grains for: a) *N*=1521 and b) *N*=14776.

As for the pulse duration influence on the etching quality, Figure 10 and Figure 11 present SEM micrographs of the traces etched by 25 and 124 fs pulses for the superposition of 15,000 pulses. The traces morphology is similar, but the shorter pulses produce better defined edges. This is probably the result of a more intense phase explosion resulting from the higher fluences required for ablation by the 124 fs pulses. Moreover, the edge of the trace etched by the shorter pulses exhibits a transition zone in which ripples can be observed. These conditions must be taken into account when machining the AISI 1045 steel with ultrashort pulses.

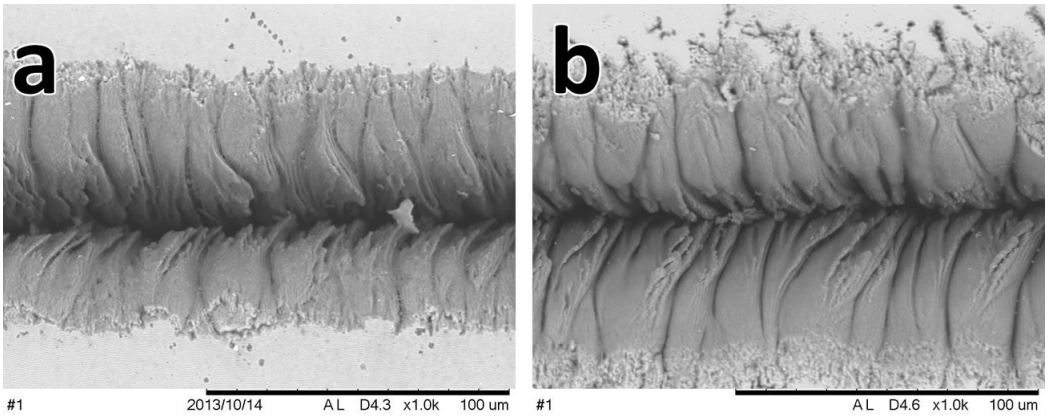

Figure 10. Micrographs of D-Scan traces etched around the χ position by a) 25 fs pulses, *N*=14,776; b) 124 fs pulses, *N*=15,955.

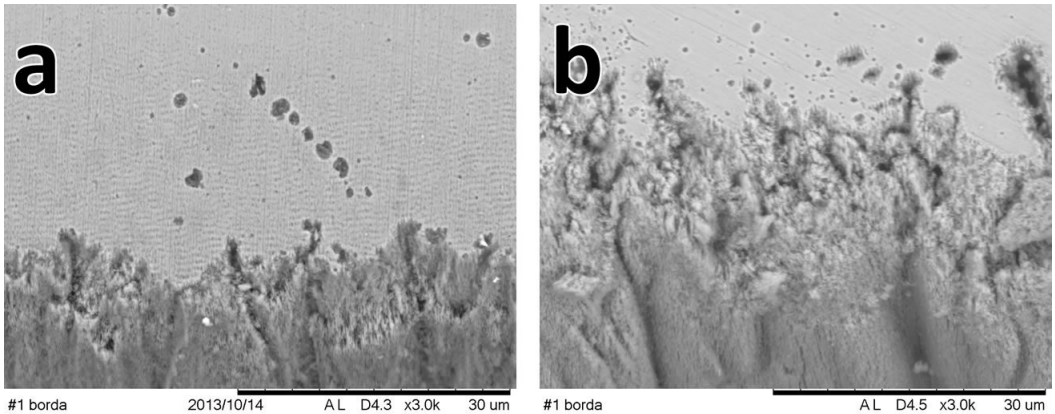

Figure 11. Magnification of the edges of the D-Scan traces shown in Figure 10 for a) 25 fs pulses, *N*=14,776; b) 124 fs pulses, *N*=15,955.

4. CONCLUSIONS

The D-Scan is a fast and simple method to determine the ultrashort pulses ablation threshold and to study the effect of the pulses superposition on it. It took us less than 2 hours of laboratory time to use this technique on AISI 1045 carbon steel to obtain a large and detailed amount of data spanning four orders of magnitude of pulses superposition, for three different pulses durations. A comparison of these set of data with the theoretical model shows a slight deviation, and a more detailed theoretical study to correctly describe the experimental results is required. The measured data also evidenced that the ablation parameters, F_{th} and S, increase as the pulses get longer.

Compared to the traditional method, the D-Scan is advantageous for determining the ablation threshold for machining purposes, once it is done in a moving sample and reproduces the machining conditions and morphology. Within this context, many ablation thresholds and machining morphologies depending on the pulses superposition were observed, allowing one to choose the most adequate processing parameters to etch the AISI 1045 steel. Besides, other subsidiary results show that the precise control of the process is possible in order to change this material surface optical properties. It is also shown that shorter pulses (25 fs) are more adequate to produce precise cuttings in this steel.

Additionally, using the AISI 1045 steel high sensitivity to thermal effects, we demonstrated that even at high superpositions (N>10,000 pulses) the HAZ, if existent, is confined within a few micrometers of the etching edge, and that outside the etched region the temperature remained below 704 °C (phase transition temperature).

REFERENCES

[1] Gad-el-Hak, M., [MEMS: introduction and fundamentals: the MEMS handbook] CRC Press/Taylor & Francis, Boca Raton(2006).

[2] Stuart, B., Feit, M., Rubenchik, A., Shore, B. and Perry, M., "Laser-Induced Damage in Dielectrics with Nanosecond to Subpicosecond Pulses," Phys. Rev. Lett., 74(12), 2248-2251 (1995).

[3] Samad, R. E., Machado, L. M., Vieira Jr, N. D. and Rossi, W. d., "Ultrashort Laser Pulses Machining" in [Laser Pulses - Theory, Technology, and Applications] InTech, 143-174 (2012).

[4] Reif, J. and Costache, F., "Femtosecond laser interaction with solid surfaces: explosive ablation and self-assembly of ordered nanostructures" in [Advances in Atomic Molecular, and Optical Physics, V. 53] Elsevier Academic Press Inc, San Diego, 227-251 (2006).

[5] Stoian, R., Rosenfeld, A., Ashkenasi, D., Hertel, I. V., Bulgakova, N. M. and Campbell, E. E. B., "Surface charging and impulsive ion ejection during ultrashort pulsed laser ablation," Phys. Rev. Lett., 88(9), 097603 (2002).

[6] Lorazo, P., Lewis, L. J. and Meunier, M., "Short-pulse laser ablation of solids: From phase explosion to fragmentation," Phys. Rev. Lett., 91(22), 225502 (2003).

[7] Perez, D. and Lewis, L. J., "Molecular-dynamics study of ablation of solids under femtosecond laser pulses," Phys. Rev. B, 67(18), 184102 (2003).

[8] Zhigilei, L. V., "Dynamics of the plume formation and parameters of the ejected clusters in short-pulse laser ablation," Appl. Phys. A-Mat. Sci. Proc., 76(3), 339-350 (2003).

[9] Du, D., Liu, X., Korn, G., Squier, J. and Mourou, G., "Laser-induced breakdown by impact ionization in $Si0_2$ with pulse widths from 7 ns to 150 fs," Appl. Phys. Lett., 64(23), 3071-3073 (1994).

[10] Stuart, B. C., Feit, M. D., Herman, S., Rubenchik, A. M., Shore, B. W. and Perry, M. D., "Nanosecond-to-femtosecond laser-induced breakdown in dielectrics," Phys. Rev. B, 53(4), 1749-1761 (1996).

[11] Bloembergen, N., "Laser-induced electric breakdown in solids," IEEE J. Quantum Elec., QE10(3), 375-386 (1974).

[12] Kanavin, A. P., Smetanin, I. V., Isakov, V. A., Afanasiev, Y. V., Chichkov, B. N., Wellegehausen, B., Nolte, S., Momma, C. and Tunnermann, A., "Heat transport in metals irradiated by ultrashort laser pulses," Phys. Rev. B, 57(23), 14698-14703 (1998).

[13] Singh, N., "Relaxation between electrons and surface phonons of a homogeneously photoexcited metal film," Pramana-J. Phys., 63(5), 1083-1087 (2004).

[14] Keldysh, L. V., "Ionization in the field of a strong electromagnetic wave," Sov. Phys. JETP-USSR, 20(5), 1307-1314 (1965).

[15] Kautek, W., Kruger, J., Lenzner, M., Sartania, S., Spielmann, C. and Krausz, F., "Laser ablation of dielectrics with pulse durations between 20 fs and 3 ps," Appl. Phys. Lett., 69(21), 3146-3148 (1996).

[16] Mero, M., Clapp, B., Jasapara, J. C., Rudolph, W., Ristau, D., Starke, K., Kruger, J., Martin, S. and Kautek, W., "On the damage behavior of dielectric films when illuminated with multiple femtosecond laser pulses," Opt. Eng., 44(5), 051107 (2005).
[17] Costache, F., Eckert, S. and Reif, J., "Near-damage threshold femtosecond laser irradiation of dielectric surfaces: desorbed ion kinetics and defect dynamics," Appl. Phys. A-Mat. Sci. Proc., 92(4), 897-902 (2008).
[18] Courrol, L. C., Samad, R. E., Gomes, L., Ranieri, I. M., Baldochi, S. L., de Freitas, A. Z. and Vieira, N. D., "Color center production by femtosecond pulse laser irradiation in LiF crystals," Opt. Expr., 12(2), 288-293 (2004).
[19] Jee, Y., Becker, M. F. and Walser, R. M., "Laser-Induced Damage on Single-Crystal Metal-Surfaces," J. Opt. Soc. Am. B, 5(3), 648-659 (1988).
[20] Ashkenasi, D., Lorenz, M., Stoian, R. and Rosenfeld, A., "Surface damage threshold and structuring of dielectrics using femtosecond laser pulses: the role of incubation," Appl. Surf. Sci., 150(1-4), 101-106 (1999).
[21] Martin, S., Hertwig, A., Lenzner, M., Krüger, J. and Kautek, W., "Spot-size dependence of the ablation threshold in dielectrics for femtosecond laser pulses," Appl. Phys. A-Mat. Sci. Proc., 77(7), 883-884 (2003).
[22] Samad, R. E. and Vieira, N. D., "Geometrical method for determining the surface damage threshold for femtosecond laser pulses," Las. Phys., 16(2), 336-339 (2006).
[23] Samad, R. E., Baldochi, S. L. and Vieira Jr, N. D., "Diagonal scan measurement of Cr:LiSAF 20 ps ablation threshold," Appl. Opt., 47(7), 920-924 (2008)
[24] Machado, L. M., Samad, R. E., de Rossi, W. and Vieira Junior, N. D., "D-Scan measurement of ablation threshold incubation effects for ultrashort laser pulses," Opt. Expr., 20(4), 4114-4123 (2012).
[25] Wolfram Research Inc., "Jacobi theta function ϑ_3," 10 December 2013, http://functions.wolfram.com/EllipticFunctions/EllipticTheta3/06/01/03/
[26] Elmer, J. W., Palmer, T. A., Babu, S. S., Zhang, W. and DebRoy, T., "Direct observations of austenite, bainite, and martensite formation during arc welding of 1045 steel using time-resolved X-ray diffraction - Phase transformations were tracked in real time using a synchrotron accelerator," Weld. J., 83(9), 244S-253S (2004).
[27] Kirkwood, S. E., van Popta, A. C., Tsui, Y. Y. and Fedosejevs, R., "Single and multiple shot near-infrared femtosecond laser pulse ablation thresholds of copper," Appl. Phys. A-Mat. Sci. Proc., 81(4), 729-735 (2004).
[28] Byskov-Nielsen, J., Savolainen, J.-M., Christensen, M. S. and Balling, P., "Ultra-short pulse laser ablation of metals: threshold fluence, incubation coefficient and ablation rates," Appl. Phys. A-Mat. Sci. Proc., 101(1), 97-101 (2010).
[29] Di Niso, F., Gaudiuso, C., Sibillano, T., Mezzapesa, F. P., Ancona, A. and Lugarà, P. M., "Influence of the Repetition Rate and Pulse Duration on the Incubation Effect in Multiple-Shots Ultrafast Laser Ablation of Steel," Phys. Procedia, 41, 698-707 (2013).
[30] Xiao, S., Gurevich, E. L. and Ostendorf, A., "Incubation effect and its influence on laser patterning of ITO thin film," Appl. Phys. A-Mat. Sci. Proc., 107(2), 333-338 (2012).
[31] Anghel, I., Jipa, F., Andrei, A., Simion, S., Dabu, R., Rizea, A. and Zamfirescu, M., "Femtosecond laser ablation of TiO_2 films for two-dimensional photonic crystals," Opt. Laser Technol., 52, 65-69 (2013).
[32] Liu, J. M., "Simple technique for measurements of pulsed Gaussian-beam spot sizes," Opt. Lett., 7(5), 196-198 (1982).
[33] Machado, L. M., [Microusinagem de dielétricos com pulsos laser de femtossegundos], Doctorate Thesis, Universidade de São Paulo, São Paulo (2012).
[34] Vander Voort, G. F., [Metallography and microstructures] ASM International, Materials Park, Ohio(2004).